

FRACTURE MECHANISM AND MICROMECHANICAL ANALYSIS OF POLYSYNTHETICALLY TWINNED CRYSTALS OF γ -TiAl ALLOYS

Y.G.Zhang, Y.H.Lu, G.K.Hu* and C.Q.Chen

Department of Materials Science and Engineering,

Beijing University of Aeronautics and Astronautics University, Beijing 100083, China

** Department of Applied Mechanics,*

Beijing Institute of Technology, Beijing 100081, China

ABSTRACT The fracture behavior and mechanism of PST crystals of a Ti-49% (mole fraction) Al alloy have been studied by using in-situ straining and micromechanical calculation. The three-dimensional micromechanical model representing the structure of PST crystal has been built, and the stress distribution ahead of the sharp and blunt crack tips either parallel to lamellar interface or perpendicular to the lamellae has been calculated by using finite element method based on linear elasticity of PST crystals. The experimental results show that the fracture behaviors and mechanisms are strongly dependent on the angle of loading axis to the lamellae. The calculation indicates that nucleation and propagation of microcrack along the interfaces are controlled by the normal stress and translamellar microcrack is controlled by shear stress ahead of crack tip.

Key words TiAl alloy PST crystal fracture behavior mechanism micromechanical model finite element method

1 INTRODUCTION

Gamma titanium aluminide has received increasing attention because of its high specific strength and stiffness at room and elevated temperature, combined with satisfactory creep behavior and adequate oxidation resistance^[1]. Ti-rich γ -TiAl based alloys have good prospects for application in the aerospace and automobile industries^[2]. The relationships between microstructures and mechanical properties of Ti-rich γ -TiAl based alloys have been known more and more clearly. Among the four types of microstructures formed by different hot-works and heat treatments, it has been recognized that the lamellar structure consisting of γ -TiAl and α_2 -Ti₃Al plates possesses higher fracture toughness, temperature strength and creep behavior, but lower ductility than others^[3]. The experimental studies of polysynthetically twinned (PST) crystals have also shown that the mechanical proper-

ties of the lamellar structure, including strength, ductility and fracture toughness, are highly anisotropic, depending on the angle of loading axis to the lamellae. The effect of grain size and lamellar spacing on the mechanical properties have been addressed more recently^[4-6]. It is necessary to carry out a systematic study of deformation and fracture processes and their mechanisms and relationships with microstructure constitutions such as grain size and lamellar spacing, and micro-mechanical analysis so that the high anisotropy in the lamellar structure may be optimized through microstructure control and alloy design in the polycrystal alloy.

Fracture behavior of the lamellar structure has been studied by many researchers. The high anisotropy behavior of fracture of PST crystals depending on their notch orientation with respect to the lamellar boundaries and crystal orientation of the lamellae was first proved by Yokoshima and Yamaguchi using three-point bending tests of specimens which are notched, fatigue-pre-

cracked and side-grooved^[4]. Chan and Kim have investigated the relationships of slip morphology, microcracking and fracture resistance in TiAl alloys with fully lamellar structure by J testing^[7,8]. These studies focused on the relationship between lamellar structure, slip and fracture behavior and mechanism, but the effect of mechanics on the fracture process is seldom referred to. The present work is focusing on fracture behavior and mechanism of PST crystals of Ti-49% (mole fraction) Al alloy by both in-situ tension testing and micromechanical modeling.

2 EXPERIMENTAL PROCEDURE AND RESULTS

PST crystal of Ti-49% (mole fraction) Al was grown at a speed of 5 mm/h in an induction floating zone furnace under argon protection. In-situ tensile specimens were cut from the PST crystals with the tensile axis near parallel, perpendicular and at an intermediate angle to the lamellae and then mechanically and electrically polished. The specimen has a gauge length of 5 mm and a cross section of 2.5 mm \times 0.8 mm. The lamellae of PST crystal grown at this speed has a thickness of 0.5 ~ 2 μ m, and Ti₃Al lamellae with an average thickness of 0.5 μ m are separated by several γ lamellae with an average thickness of 1.1 μ m. In-situ straining experiment was conducted in a JSM-5800 scanning

electron microscope (SEM) equipped with a JEOL tensile stage, and the crack path and microcrack nucleation were observed and recorded during the in-situ tests. The results are summarized as follow.

2.1 Tensile axis nearly perpendicular to lamellae

When the tensile axis was nearly perpendicular to the lamellae, the crack nucleated parallel to the lamellae, kept sharpness and propagated along the interface, as shown in Fig. 1. No extrinsic toughness mechanisms were noted to affect the crack tip.

2.2 Tensile axis nearly parallel to lamellae

When the tensile axis was nearly parallel to the lamellae, the crack-tip perpendicular to the lamellae nucleated and was soon blunted, then its propagation stopped presumably because of interface sliding, as can be seen in Fig. 2 (a). Abundant microcracks nearly perpendicular to the $\gamma/\alpha_2/\gamma$ lamellae were nucleated in the area both ahead of and besides the main crack, forming a diffuse microcrack zone, as shown in Fig. 2 (b). Upon increasing stress level, the existing microcracks opened to a different extent and linked with each other by delamination of interface or tearing, and new microcracks nucleated ahead of existing microcracks and grew continuously, eventually some linked microcracks propa-

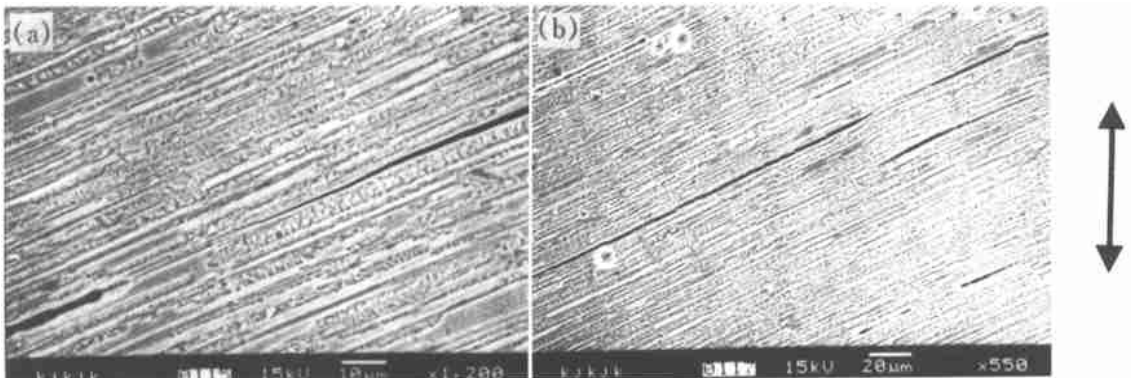


Fig. 1 Crack propagation along lamellar interfaces with tensile axis nearly perpendicular to lamellae
(a)—Main crack along interface; (b)—Microcrack-cracks parallel to interfaces

(double arrows indicates loading direction)

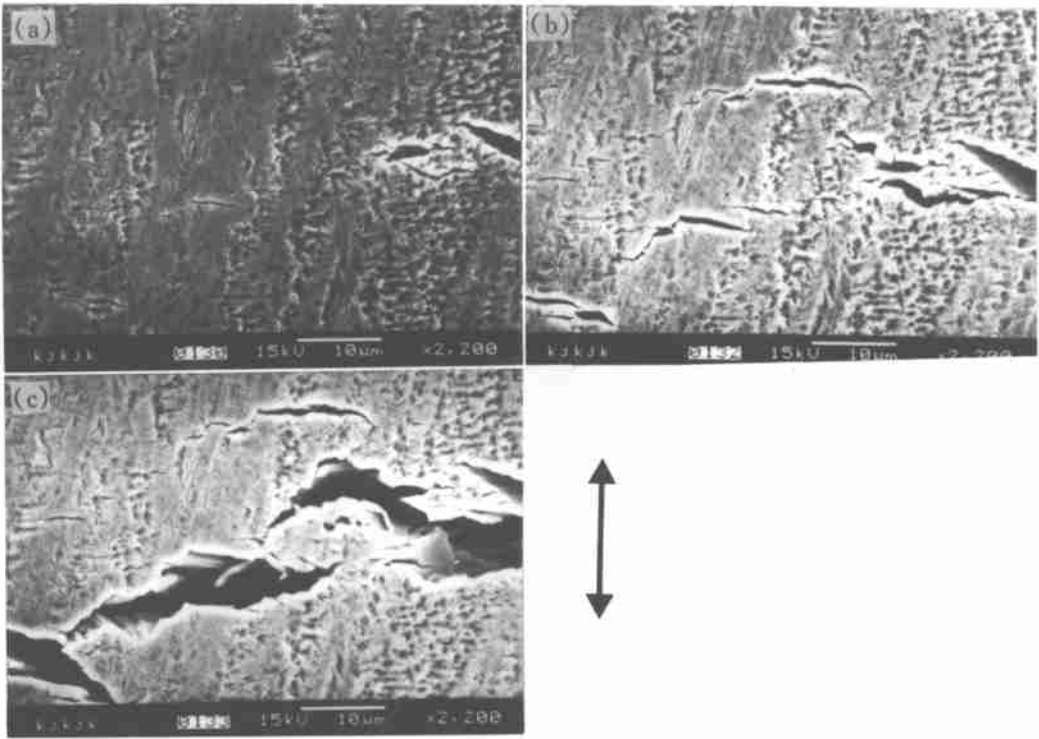


Fig. 2 Crack propagation process of specimen loaded with axis nearly parallel to lamellae
 (a)—Microcracks at ahead of main crack; (b)—Growth of microcracks;
 (c)—Linkage between main crack and microcracks

gated and linked to the main crack, as shown in Fig.2(c). In this way, thus the main crack propagated forward.

2.3 Tensile axis inclined at intermediate angle to lamellae

When the tensile axis was inclined at an intermediate angle to the lamellae, the main crack propagated in an alternate mode between the delamination and translamellae. When the angle between tensile axis and lamellae was relatively large (for example, $\sim 56^\circ$ in Fig.3(a)), the interface delamination was dominant in this process since a few microcracks parallel to the interface were always found to form first around the area ahead of the main crack-tip, and the main crack propagated forward by tearing or shear of the ligament across the lamellae. When the angle between tensile axis and lamellae was relatively small (for example, $\sim 20^\circ$ in Figs. 3(b)~(d)),

the dominant fracture mode became translamellae. A few microcracks nearly normal to the lamellae ahead of the main crack tip formed first in the diffuse zone (Fig. 3 (b)), some of which linked each other or linked with main crack through delamination of the lamellae (Fig. 3(c)) or crack deflection (Fig. 3(d)), the main crack propagating forward in this way.

3 MICROMECHANICAL MODELING

It has been well known that the lamellar structure is composed of α_2 -Ti₃Al (DO₁₉ structure) and γ -TiAl (L1₀ structure) lamellae with the orientation relationships of $\{110\}\gamma // (0001)\alpha_2$ and $\langle 110 \rangle \gamma // \langle 1120 \rangle \alpha_2$. There are six possible relationships between γ -TiAl and α_2 -Ti₃Al plates^[9],

$[110]\gamma \uparrow \uparrow [1120]\alpha_2$, $[110]\gamma \uparrow \uparrow [1210]\alpha_2$,

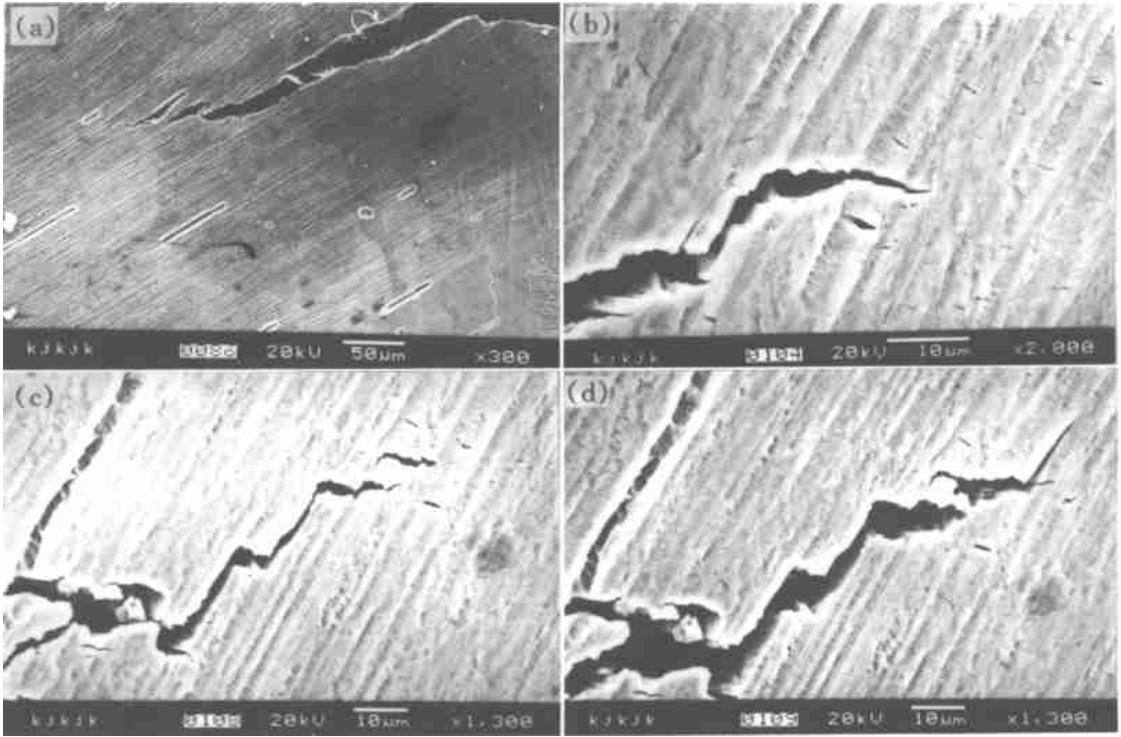


Fig 3 Crack propagation process of specimen with tensile axis inclined at intermediate angle to lamellae

- (a)—Delamination was dominant with relatively large angle ($\sim 56^\circ$);
 (b)~(d)—Translamellae dominant with relatively small angle ($\sim 20^\circ$)

$[\bar{1}10]_\gamma \uparrow \uparrow [\bar{2}110]_{\alpha_2}$, $[\bar{1}10]_\gamma \uparrow \downarrow [\bar{1}120]_{\alpha_2}$,
 $[\bar{1}10]_\gamma \uparrow \downarrow [\bar{1}210]_{\alpha_2}$, $[\bar{1}10]_\gamma \uparrow \downarrow [\bar{2}110]_{\alpha_2}$.

Six orientation relationships also exist between two neighboring γ ordered domains if the slight tetragonality of TiAl phase is ignored, (a) $[\bar{1}10] \uparrow \uparrow [\bar{1}10]$, (b) $[\bar{1}10] \uparrow \uparrow [\bar{1}01]$, (c) $[\bar{1}10] \uparrow \uparrow [\bar{0}11]$, (d) $[\bar{1}10] \uparrow \downarrow [\bar{1}10]$, (e) $[\bar{1}10] \uparrow \downarrow [\bar{1}01]$, (f) $[\bar{1}10] \uparrow \downarrow [\bar{0}11]$, where $\uparrow \uparrow$ and $\uparrow \downarrow$ mean parallel and antiparallel respectively. (d) represents a true-twin relationship, (e) and (f) present an pseudo-twin relationship, (b) and (c) show the neighboring γ -TiAl ordered domains having 120° rotational boundary, while translation order-fault interface may form in (a).

The 120° -rotational ordered domain also exists in each of γ lamellae, forming $(011)_\gamma$ type

antiphase boundaries. The antiphase boundary can be related simply by mutual perpendicular of the c -axis in the $(011)_\gamma // (101)_\gamma$ twin-related regions. In general each domain has an average length of about $35\mu\text{m}$ determined by examining TEM micrographs of the crystals.

Considering the periodical feature of structure of PST crystal and referring to other works^[10], we described our three-dimensional micromechanical model in the following sketch map, shown in Fig.4(a). The model was constructed by taking γ_1 as a matrix orientation as shown in Fig. 4(b) and other γ_n plates being rotated by $(n-1) \times 60^\circ$ to the γ_1 consequently. Six types of domains $\gamma_1, \gamma_2, \gamma_3, \gamma_4, \gamma_5, \gamma_6$ possess the definite crystallographic relationships described as above and the relationship may be expressed as

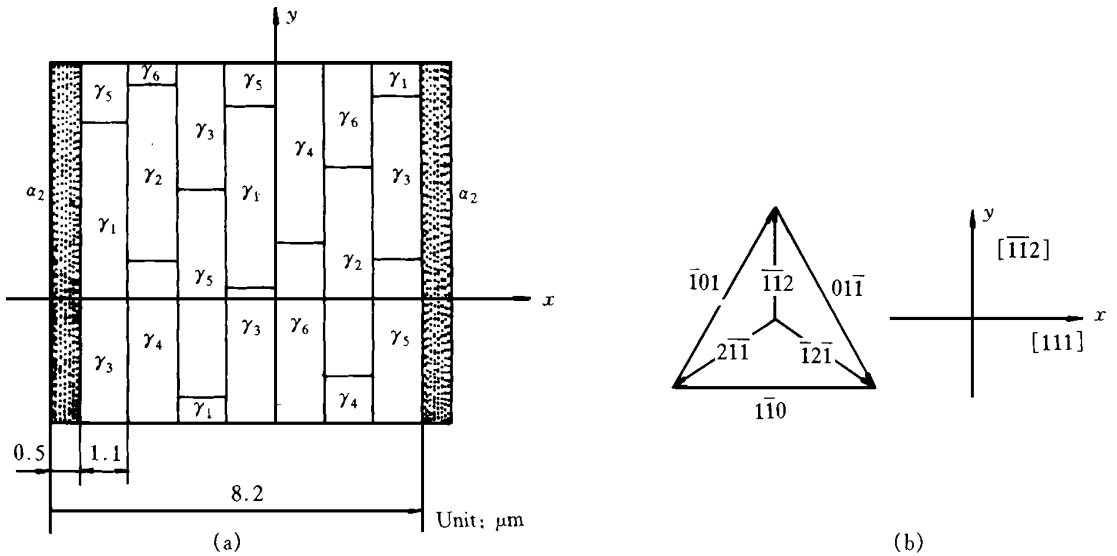


Fig. 4 Micromechanical modeling

(a)—Sketch three-dimensional micromechanical model; (b)—Orientation of γ_1

$$\gamma_n = M\gamma_1, n = 1, 2, 3, 4, 5, 6.$$

Here M is transition matrix,

$$M = \begin{bmatrix} 2/3 & -1/3 & 2/3 \\ 2/3 & 2/3 & -1/3 \\ -1/3 & 2/3 & 2/3 \end{bmatrix}^{n-1}$$

There exist three types of boundaries along the x axis, i. e., true-twin relation boundary γ_1/γ_4 , γ_3/γ_6 , γ_2/γ_5 ; pseudo-twin relation boundary γ_4/γ_5 , γ_2/γ_6 ; and 120° rotational boundary γ_3/γ_5 . 120° -rotational ordered domain boundaries within each of γ lamellae have been also taken into account.

The stress distribution ahead of crack-tip of following two conditions has been calculated using finite element program ANSYS 5.3 on the basis of linear elasticity theory. One condition is that the crack is parallel to the lamellae and the lamellae is perpendicular to the tensile loading axis; the other is that the crack is perpendicular to the lamellae and the lamellae is parallel to the tensile axis. The boundary condition of the calculation is unidirectional tensile perpendicular to the crack plane. The elastic constants used in present calculation are listed in Table 1^[11].

Table 1 Elastic constants in GPa of TiAl and Ti₃Al

Alloy	C_{11}	C_{33}	C_{12}	C_{13}	C_{44}	C_{66}
TiAl	190	185	105	90	120	50
Ti ₃ Al	221	238	71	85	69	75

lamellar boundary in the x - y plane (z axis is into the paper) when the lamellae are perpendicular to the tensile axis. The crack-tip is arranged in at $x=0$, $y=0$. Figs.5(a) ~ (c) show the maps of iso-stress line representing the normal stress S_1 , shear stress S_{INT} and von Mises effective stress S_{EQV} ahead of the crack-tip respectively. Here

$$S_{EQV} = \{ [(\sigma_x - \sigma_y)^2 + (\sigma_z - \sigma_x)^2 + (\sigma_y - \sigma_z)^2]^{1/2} + 3(\tau_{xy}^2 + \tau_{yz}^2) + \tau_{xz}^2 \}^{1/2}$$

It can be seen that the maximum normal stress S_1 is located at the crack-tip, the maximum shear stress S_{INT} and the von Mises effective stress S_{EQV} are in one side of the crack-tip. It could be predicated that the crack propagation along the interface might be controlled by the

Fig. 5 shows a sharp crack tip formed along

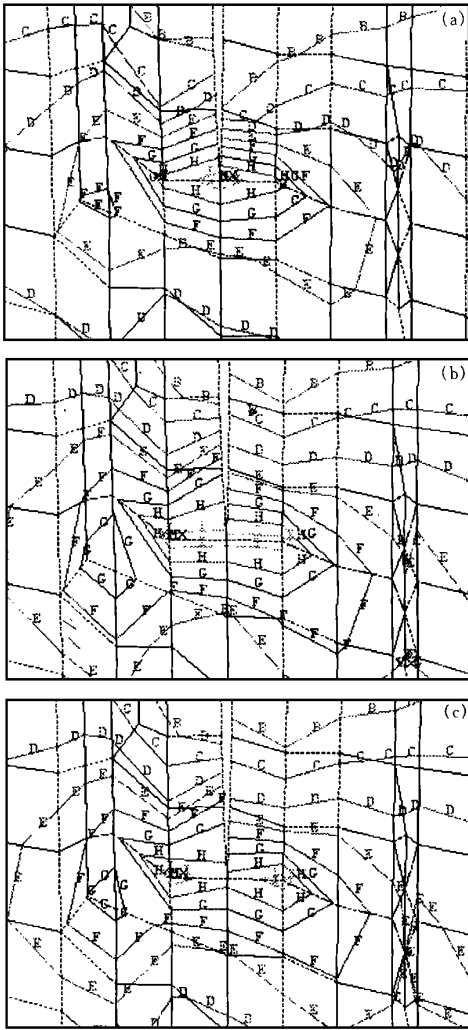


Fig. 5 Distribution of stress ahead of sharp crack tip formed along lamellar interface with loading axis perpendicular to lamellae
 (a)—Normal stress S_I ; (b)—Shear stress S_{INT} ;
 (c)—von Mises effective stress S_{EQV}
 (MX marks the maximum stress location)

normal stress of the crack-tip in this condition.

Fig. 6 represents a sharp crack tip perpendicular to the lamellae in the x - y plane when the lamellae are parallel to the tensile axis. The crack-tip is located in the boundary between γ_5 and γ_3 domains which have an 120° rotational relationship. Figs. 6(a) ~ (c) show the maps of

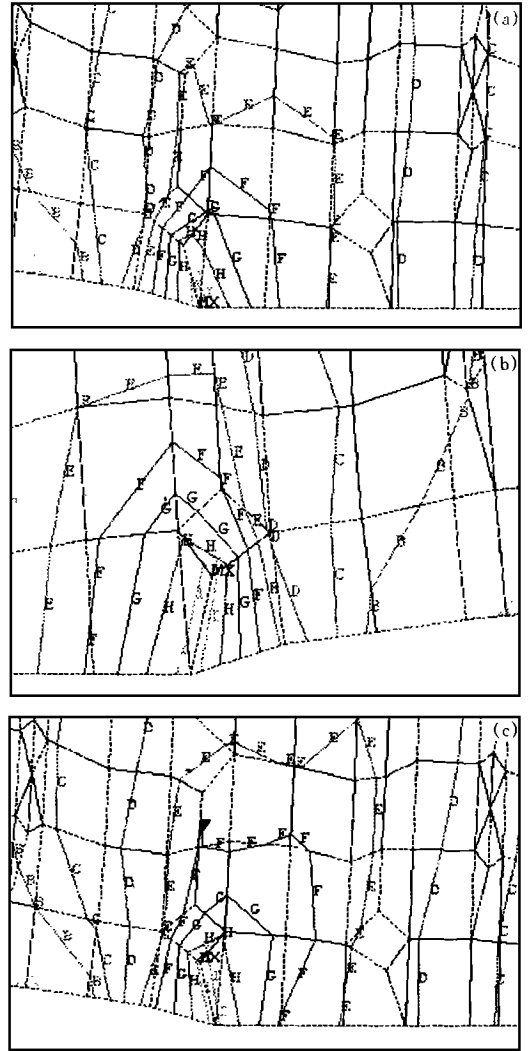


Fig. 6 Distribution of stress ahead of sharp crack tip perpendicular to lamellae with tensile axis parallel to lamellae
 (a)—Normal stress S_I ; (b)—Shear stress S_{INT} ;
 (c)—von Mises effective stress S_{EQV}

iso-stress lines representing the normal stress S_I , shear stress S_{INT} and von Mises effective stress S_{EQV} in this condition respectively. Similar to above condition, the maximum normal stress S_I is located at the crack-tip and the other two maximums distribute in both sides of the crack tip. Under this circumstance, combining with the experimental results, we believe that

the crack propagation and microcrack nucleation are controlled by the shear stress ahead of the crack tip.

4 DISCUSSION

The in-situ straining experiment clearly shows that the microcrack nucleation and crack path of PST crystals are strongly dependent on the angle of loading axis to the lamellae. The micromechanical modeling results indicate that the crack propagation and microcrack nucleation under the two conditions considered are controlled by different mechanisms.

When the tensile axis is nearly perpendicular to the lamellae, crack-tip parallel to the lamellae is only controlled by uniaxial tensile perpendicular to the crack plane, and the crack propagates through interface delamination controlled by the maximum normal stress which is located at the crack tip. In this condition, in general, the crack-tip keeps sharpness according to our observation. When the crack tip bluntness is taken into account, it is found that the maximum normal stress is still located at the crack tip, as shown in Fig. 7(a). Thus the main crack propagates forward along the interface boundary and no extrinsic toughness mechanism has an effect on the crack tip, which leads to low fracture toughness.

When the tensile axis is nearly parallel to the lamellae, crack-tip perpendicular to the lamellae is also controlled by uniaxial tensile perpendicular to the crack plane. In this case, however, the maximum normal stress located at the main crack tip can not push the crack across the interfaces. By considering the experimental observation, it is reasonable to consider the role of the shear stress distributing at both side of the crack tip in the nucleation of the microcracks. According to Stroh's theory^[12], the microcrack nucleation induced by dislocation pile-up in γ lamellae is controlled by only shear stress, and the microcrack nucleation plane should lie at about 70.5° from the slip plane. If it is assumed that $\langle 110 \rangle$ direction of the γ plates are perpendicular to loading axis, the slip planes across the interface lying at an angle of 70° to the interface

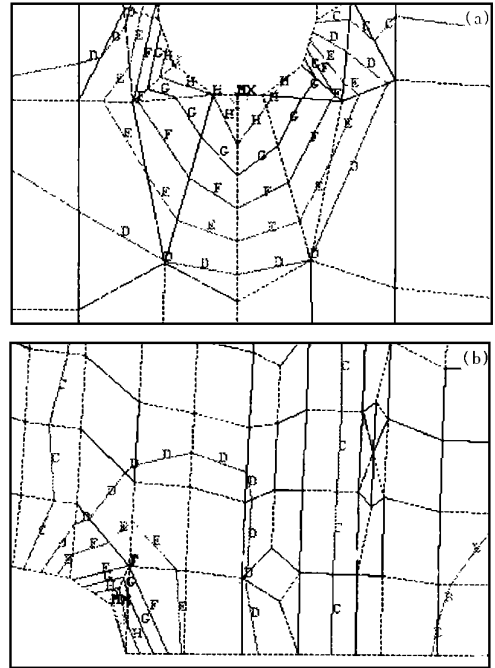


Fig. 7 Distribution of stress ahead of blunted crack-tip
 (a)—Normal stress distribution of crack-tip along lamellar interface with tensile axis perpendicular to lamellae; (b)—Shear stress distribution of crack-tip perpendicular to lamellae with tensile axis parallel to lamellae

may exist. When the dislocation pile-up on these slip planes occurred under the shear stress ahead of the crack-tip, a normal stress due to the dislocation pile-up may be built up and has a maximum value in the direction nearly parallel to the lamellae, and shear stress parallel to the interface of dislocation pile up was slack because of interface sliding^[9]. So under effect of the normal stress parallel to the lamellae, the cleavage might occur in the adjacent lamella first on the planes perpendicular to the lamellae such as (100), (001) and (110), not on the slip planes such as (111) plane because of small difference in cleavage energy between (100), (001), (110) and slip plane (111)^[11]. The experimental fact that the microcrack nucleation plane nearly perpendicular to lamellae may be explained on the basis

of the assumption. When the crack tip is blunted at the interfaces, the site of the maximum shear stress ahead of crack-tip shifts to the blunted crack-tip (see Fig. 7(b)) and the diffuse zone of the microcracks shifts to the crack tip simultaneously. Thus, the main crack propagates by nucleation, coalescence and linkage of the microcracks perpendicular to the lamellae. During this procedure various toughness mechanisms such as crack-tip blunting, microcracking, crack deflection and shear ligament have strong effect on propagation of the crack-tip, leading to high resistance of crack propagation.

When the tensile axis is inclined at an intermediate angle from the lamellae, the main crack propagates in the alternate mode between interface delamination and translamellar crack. When the angle is relatively large, the normal stress ahead of crack-tip is dominant and causes the interface delamination first in the interfaces because of stress asymmetry, which forms the shear ligament, the main crack propagates by tearing and shearing the ligament, leading to a little high fracture toughness. When the angle is relatively small, the shear stress would be dominant and first causes the microcrack nucleation normal to the lamellae in the microcrack diffuse zone, and the crack-tip might deflect back and forth between interface delamination and translamellae. During this procedure deflection of the main crack, formation of a diffuse zone of microcracks and bridge ligament would be expected, leading to a rough fracture surface and a high resistance of crack propagation.

5 CONCLUSIONS

The crack propagation path and microcrack

nucleation mechanisms of PST crystal of γ -TiAl base alloys are strongly dependent on the angle of loading axis to the lamellae and clearly related to the toughness mechanisms and crack propagation resistance. The normal stress ahead of the crack tip plays an important role in nucleation of microcrack along interface, but translamellar microcrack is controlled by shear stress ahead of the crack-tip.

ACKNOWLEDGMENTS The authors would like to thank the National Natural Science Foundation of China for its financial support.

REFERENCES

- 1 Young-Won Kim and Dennis M. Dimiduk, *JOM*, 40 (1991).
- 2 Blair London, D. L. Larsen Jr., D. A. Wheeler, and P. R. Aime, in: *Structural Intermetallics*, edited by R. Darolia, J. J. Lewandowski, C. T. Liu *et al*, TMS, 151(1993).
- 3 Young-Won Kim, *JOM*, 30(January 1994).
- 4 S. Yokoshima and M. Yamaguchi, *Acta Mater.*, 44, 873(1996).
- 5 Y. Umakoshi and T. Nakano, *Acta metall. mater.*, 41, 1155(1993).
- 6 K. S. Chan and Y.-W. Kim, *Acta metall. mater.*, 43, 439(1995).
- 7 K. S. Chan and Y.-W. Kim, *Mater. Metall. Trans. A*, 25A, 1217(1994).
- 8 Young-Won Kim, *Mater. Sci. Eng.*, A192/193, 519(1995).
- 9 H. Inui, M. H. Oh, A. Nakamura and M. Yamaguchi, *Phil. Mag. A*, 66, 539(1992).
- 10 Sabine M. Schlogl and Franz D. Fischer, *Phil. Mag. A*, 75, 621(1997).
- 11 M. H. Yoo, J. Zou and C. L. Fu, *Mater. Sci. and Eng.*, A 192/193, 14(1995).
- 12 Stroh A. N., *Proc. Roy. Soc.*, 223A, 404(1954); 232A, 548(1955).